Effect of Orientation and Aspect Ratio of an Internal Flat Plate on Natural Convection in a Circular Enclosure

Authors:

Anjie Wang, Cunlie Ying, Yingdong Wang, Lijun Yang, Yunjian Ying, Lulu Zhai, Wei Zhang

Abstract:

This work presents a numerical investigation on natural convection in a circular enclosure with an internal flat plate at Ra = 106. The cross-section area of the plate was fixed at three values, H·W/D2 = 0.01, 0.04, and 0.09, in which H and W are the height and width of the plate and D is the diameter of the enclosure while the aspect ratio changes, which makes the plate vertically placed (H > W) or horizontally placed (H < W). The objective of this work was to explore the effects of the orientation and aspect ratio of the plate on the characteristics of natural convection in various aspects. The numerical results reveal that the overall heat transfer rate is higher for the vertically placed plate and increases with the cross-section area, while the width of the plate has almost no effect for the horizontally placed plate, especially for the plate with a relatively large cross-section area. Depending on the orientation and aspect ratio, there can be one primary vortex, one primary and one secondary vortex, or one secondary and two separated vortices to each side of the plate, and the thermal plume structure may appear at the sharp top corners of the plate. Consequently, local heat transfer on the surfaces of the enclosure and plate is affected. Synergy analysis reveals that the enhancement of heat transfer from the fluid circulation is the most significant at the center of the vortices and at the boundary between them.

Article

Effect of Orientation and Aspect Ratio of an Internal Flat Plate on Natural Convection in a Circular Enclosure

Anjie Wang [1,2], Cunlie Ying [3], Yingdong Wang [3], Lijun Yang [3], Yunjian Ying [3], Lulu Zhai [1,2] and Wei Zhang [1,2,*]

[1] National-Provincial Joint Engineering Laboratory for Fluid Transmission System Technology, Zhejiang Sci-Tech University, Hangzhou 310018, Zhejiang, China; wang_st154@163.com (A.W.); zhailulu@zstu.edu.cn (L.Z.)

[2] Faculty of Mechanical Engineering and Automation, Zhejiang Sci-Tech University, Hangzhou 310018, Zhejiang, China

[3] Zhejiang Yilida Ventilator Co., Ltd., Taizhou 318056, Zhejiang, China; yingcunlie@yilida.com (C.Y.); wangyingdong@yilida.com (Y.W.); yanglijun@yilida.com (L.Y.); yingyunj@163.com (Y.Y.)

[*] Correspondence: zhangwei@zstu.edu.cn

check for updates

Abstract: This work presents a numerical investigation on natural convection in a circular enclosure with an internal flat plate at $Ra = 10^6$. The cross-section area of the plate was fixed at three values, $H \cdot W / D^2$ = 0.01, 0.04, and 0.09, in which H and W are the height and width of the plate and D is the diameter of the enclosure while the aspect ratio changes, which makes the plate vertically placed ($H > W$) or horizontally placed ($H < W$). The objective of this work was to explore the effects of the orientation and aspect ratio of the plate on the characteristics of natural convection in various aspects. The numerical results reveal that the overall heat transfer rate is higher for the vertically placed plate and increases with the cross-section area, while the width of the plate has almost no effect for the horizontally placed plate, especially for the plate with a relatively large cross-section area. Depending on the orientation and aspect ratio, there can be one primary vortex, one primary and one secondary vortex, or one secondary and two separated vortices to each side of the plate, and the thermal plume structure may appear at the sharp top corners of the plate. Consequently, local heat transfer on the surfaces of the enclosure and plate is affected. Synergy analysis reveals that the enhancement of heat transfer from the fluid circulation is the most significant at the center of the vortices and at the boundary between them.

Keywords: natural convection; flat plate; aspect ratio; orientation; vertical; horizontal

1. Introduction

Natural convection in an enclosure is a fundamental problem in many engineering applications. For example, in sand casting of a metal component, the liquid metal experiences cooling from the sand mold and weakly circulates before its solidification; for indoor air-conditioning in the winter, heaters induce fluid circulation and alter the temperature distribution in a room. In these applications, the buoyancy that drives the fluid's circulation within the enclosed space is generated by the temperature difference between either the various sidewalls of the enclosure (differentially heated enclosure) or the enclosure and the internal entity. For the latter case, the characteristics of fluid flow and heat transfer are determined by a number of factors, including the shape, size, and position of the internal entity within the enclosure; the temperature difference between the entity and the enclosure; the thermal boundary conditions, and the thermophysical properties of the fluid. The thermal and flow processes are integrated, in that the flow is induced by the temperature difference, while the circulating flow results

in mass transfer and also influences the temperature distribution. Although there have been many studies on this topic, the problem is still worthy of investigation for specific geometrical configurations considering the complex and various configurations encountered in realistic applications.

The natural convection between a cold enclosure and a hot internal thin flat plate is a model as an approximation to realistic applications. The enclosure is normally assumed have circular or rectangular geometry for production simplicity, while the internal plate can be placed by attaching to the sidewalls of the enclosure or in an isolated way. Depending on the position and orientation of the plate, the pattern of fluid circulation is different, and the heat transfer is consequently affected. Alteç and Kurtul [1] studied natural convection in a tilted rectangular enclosure with an internal isolated flat plate at $Ra = 10^5$–10^7. The enclosure has three adiabatic sidewalls and one cold sidewall, which was always parallel with the plate. It was found that for a square enclosure at a high Rayleigh number, the mean heat transfer rate increased with the tilt angle and reached a maximum at 22.5°; however, the mean heat transfer rate remained almost unchanged up to 22.5° for the enclosure with an aspect ratio of two. A similar physical configuration was also studied by Wang et al. [2]. The tilted enclosure has two adiabatic sidewalls, and two cold sidewalls, which can either be parallel with or perpendicular to the internal hot flat plate. Heat transfer is enhanced by the vertically placed plate. The effect of the two orientations of the internal plate was also studied by Öztop et al. [3] for a horizontally placed enclosure with cold left and right sidewalls at $Ra = 10^4$–10^6 by considering various sizes and positions of the plate. The mean heat transfer rate monotonically increased with the size of the plate and the increase was more notable for the vertically placed plate at all Rayleigh numbers. Tasnim and Collins [4] considered natural convection in a differentially heated square enclosure with an internal adiabatic arc-shaped plate. The length and radius of the arc were varied to explore the blockage effect on the flow and thermal behaviors. It was found that the arc modified the pattern of fluid circulation, and the modification was enhanced at small arc radius; the overall heat transfer was degraded by the introduction of the arc. For a finite-thickness rectangular plate placed within a square enclosure, Wang et al. [5] found that the distance between the plate and the sidewall of the enclosure is a critical parameter. For $Ra < 5 \times 10^5$, the overall heat transfer rate is not sensitive to the position of the plate as the distance is larger than about one fourth of the cavity width while it significantly increases with the decreasing distance as the distance is smaller than 20% of the cavity width.

There are also a number of works focusing on natural convection in an enclosure with multiple plates. The fluid circulation is confined by the plates, and the formation and interaction of recirculating vortices are complexly dependent on the geometrical parameters and thermal properties of the plates. Hakeem et al. [6] studied natural convection in a square enclosure with two heat-generating flat plates of the same size but positioned perpendicular to each other, i.e., one was vertically placed and the other was horizontally placed. The effect of the location of the plates was numerical studied. It was concluded that the overall heat transfer rate is not significantly affected by the movement of either plate as long as the plates are not wall mounted. In the condition that the enclosure surface was prescribed with a constant heat flux, the heat transfer was degraded by the upward movement of the horizontal plate but enhanced by the horizontal movement of the vertical plate. In the following work, Kandaswamy et al. [7] explored the same physical problem except for thermal boundary conditions in which the enclosure was held at a constant low temperature while the temperature of the two plates was different. They found that the heat transfer mechanism was mainly determined by the hotter plate, and the overall heat transfer rate was higher as the vertical plate was hotter than the horizontal one.

In addition to the dimension and position, the inclination of the internal plate also affects the natural convection in an enclosure. Singh and Liburdy [8] experimentally investigated the natural convection in a circular enclosure with an internal thin flat plate using the holographic interferometry technique. The authors found that the local and overall heat transfer rate is strongly affected by the inclination since the pattern of flow separation at the ends of the plate is greatly influenced. The effect of inclination is minor for angles greater than 60 degrees from the horizontal. Recently, Zhang et al. [9] numerically investigated natural convection in a circular enclosure with an internal flat plate that was

inclined and eccentrically placed. The formation and intensity of recirculating vortices are dependent on the eccentricity and inclination, and there can be up to two and three vortices in the left and right halves of the enclosure, respectively. It was found that the heat transfers in the gap between the end of the plate and the enclosure is dominated by conduction at high eccentricity.

The internal plates determine the heat transfer characteristics by changing the thermal conditions but also through modification of the fluid circulation pattern. For isolated plates placed within the enclosure, the fluid circulation is confined but not fully suppressed; however, as the plates are mounted on the walls of the enclosure, recirculating vortices may form in the corner region and greatly alter the local heat transfer performance. Dagtekin and Öztop [10] studied natural convection in an enclosure with two hot plates mounted on the bottom wall and investigated the effect of height and spacing on the heat transfer. The mean heat transfer rate increased with the height of the plate because of the increased surface area of the heating source, and the position of the plates had more of an effect on the flow than on the heat transfer. Nag et al. [11] considered an infinite thermal-conductive or adiabatic plate mounted on the hot sidewall of a differentially heated square enclosure. The authors concluded that the plate of infinite thermal conductivity always increases the overall heat transfer rate irrespective of its position or size while the adiabatic plate attenuates the heat transfer. The same physical configuration was also studied by Tasnim and Collins [12] to investigate the effects of length and position on natural convection. Two competing mechanisms were observed, which determined the patterns of fluid flow and heat transfer, i.e., the blockage effect, which depends on the length of the plate; and the heating of the fluid by the plate. For a short triangular thermal-conductive fin, Sun et al. [13] studied the mixed convection in a lid-driven cavity by mounting the fin on the hot sidewall, cold sidewall, or adiabatic bottom wall. It was found that by placing the fin on the left or right sidewall, the effect of the fin on the heat transfer performance was not only determined by its position but was also greatly dependent on the moving direction of the lid of the cavity through the interaction between the buoyancy generated by the temperature difference and viscous shear stress of the lid. However, the fin on the bottom wall had a tiny effect on the streamline and temperature distributions. The effect of natural convection on the flow in an enclosed space has also been considered in other applications [14–17].

It is summarized from the literatures reviewed above that for a hot plate in a cold enclosure, the natural convection is influenced by a number of factors, including the dimension, position, orientation, and shape of the plate, and the associated thermal boundary conditions for both the plate and enclosure. The existence of the plate affects the fluid flow and heat transfer primarily through two mechanisms. The first is the heating of fluid on the surface, which is the driving force for the fluid circulation; the second is the confinement on the fluid circulation by partially partitioning the enclosure into multiple connected sub-domains, thus the behaviors of the local evolution of vortices are greatly altered. Compared with the cylinder, the geometry of a plate is characterized by its high specific surface area, where the heating of fluid around it is more intense but may not be more effective depending on the pattern of fluid circulation, which is affected by the orientation of the plate and the confinement imposed on the fluid. At medium and high Rayleigh numbers, the local heat transfer performance is significantly lowered by the local quasi-stationary fluid in the corner region or the separated bubble. In most of the existing researches reviewed above, the plate is assumed as a zero-thickness one, which only heats the fluid and confines the flow while the effect of shape and size has not been thoroughly discussed. In this work, we performed a numerical investigation on the natural convection in a circular enclosure with an internal flat plate of various dimensions. Assuming that the plate is produced with a certain amount of material, the cross-section area is fixed but the height and width are varied. The plate is placed within the enclosure in two orientations depending on its height (H, dimension in the vertical direction) and width (W, dimension in the horizontal direction): The vertically positioned plate for $H > W$ and horizontally positioned plate for $H < W$. It is anticipated that by varying the height and width of the plate, the fluid is heated and circulates within the enclosure in various modes, resulting in different distributions of the local heat transfer rate

and recirculating vortices. The above flat plate geometry is a typical model widely encountered in engineering applications of enhanced/weakened heat transfer. For example, in the transportation of certain types of liquid in heat pipes in small- and mid-sized electronic devices, the pipe containing the liquid is normally enclosed by an outer enclosure to reduce heat exchange with the surrounding medium. The choice of the geometry of the cross-section of the heat pipe is significant and two factors have to be considered. The first is that the area of the cross-section cannot be reduced to permit a sufficient mass flow rate, thus the velocity of the internal liquid could remain constant, which facilitates the design of the accessory components. The second is that the geometry of the heat pipe is normally a rectangle to save space, which facilitates the layout of multiple heat pipes in a small space. In this condition, the maximum/minimum heat transfer rate between the heat pipe and outer enclosure is a quantity that is determined by the geometry of the heat pipe. The configuration is also employed in other applications. In heating tubes with the thin plate twined with an electric resistance wire as the thermal source, the effectiveness of heating, as measured by the heat transfer rate and uniform temperature rise in the whole enclosed space, is dependent on the position, orientation, and size of the plate. The thermal treatment of the metal component after welding is also characterized by natural convection of the internal entity in an enclosed space. The present work is a theoretical research on a flat plate of various geometries, which has not been studied before. The objective of the present study was to qualitatively and quantitatively investigate the effect of the dimensions and shape of a plate on the thermal and flow characteristics. The effects are presented and analyzed by the overall heat transfer rate, the spatial structures of isotherms and streamlines, and the distributions of the local heat transfer rate on the surfaces of the plate and enclosure. We also carried out synergy principle analysis to visualize how convection enhances heat transfer under different parameter combinations.

2. Numerical Setup

2.1. Physical Model

The configuration of the physical problem is shown in Figure 1. A flat plate was placed concentrically within a circular enclosure. The height of the plate is H and the width is W, and the radius of the circular enclosure is R and diameter is D. Depending on the values of H and W, we considered three types of plate, namely, square ($H = W$), vertically positioned ($H > W$), and horizontally positioned ($H < W$) plate. The three types were assumed to have the same cross-sectional area, i.e., constant cross-section area $H \cdot W$, with the consideration that the production of the various plates would cost the same amount of material. The surfaces of the plate and enclosure are isothermal and denoted by the higher temperature, T_i, and lower temperature, T_o, respectively. The enclosure was filled with air ($Pr = 0.71$). All simulations were performed at Rayleigh number $Ra = 10^6$, where heat transfer is dominated by natural convection. In this work, the cross-section area of the plate was chosen at $H \cdot W/D^2 = 0.01$, 0.04, and 0.09. The values for the height and width of the three types of plate are listed in Table 1 with notations clearly explained.

Table 1. Notations for the flat plate of various geometries in the present study. The first letter S, M, and L respectively denotes small, medium, and large sizes; the second letter H, V, and S respectively denotes horizontally positioned, vertically positioned, and square plates.

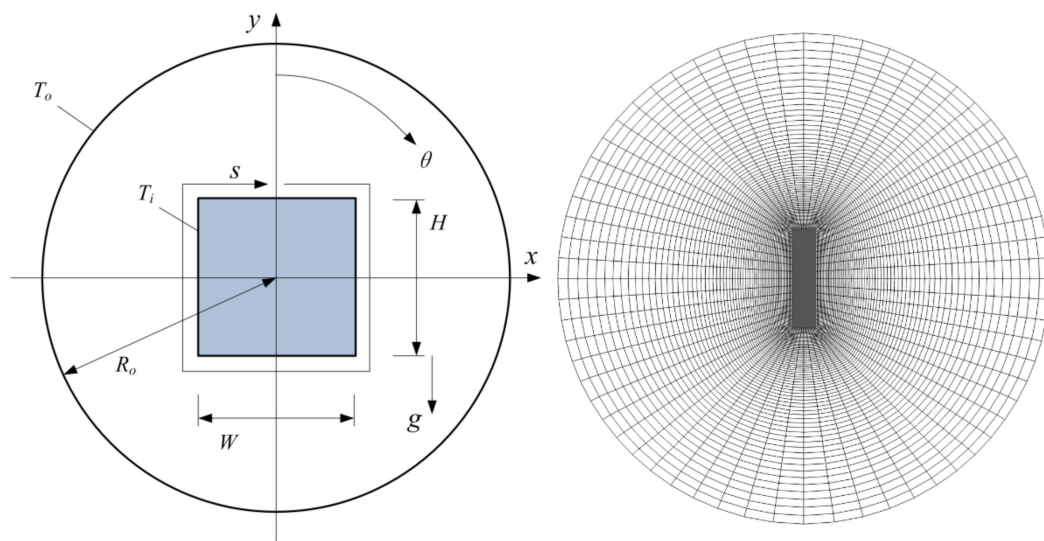| Notation	$H \cdot W/D^2$	Remark
SV	0.01	$H > W$ and $H/D = 0.2\ (0.1)\ 0.8$
SH	0.01	$H < W$ and $W/D = 0.2\ (0.1)\ 0.8$
SS	0.01	$H/D = W/D = 0.1$
MV	0.04	$H > W$ and $H/D = 0.3\ (0.1)\ 0.8$
MH	0.04	$H < W$ and $W/D = 0.3\ (0.1)\ 0.8$
MS	0.04	$H/D = W/D = 0.2$
LV	0.09	$H > W$ and $H/D = 0.4\ (0.1)\ 0.8$
LH	0.09	$H < W$ and $W/D = 0.4\ (0.1)\ 0.8$
LS	0.09	$H/D = W/D = 0.3$

Figure 1. (**Left**) Configuration of the physical problem. The height of the plate is *H* and the width is *W*; *s* is the local coordinate along the cylinder surface. (**Right**) A schematic of the structured grid for the plate at *H/D* = 0.2 and *W/D* = 0.05 (denoted as SV$_{0.2}$, i.e., Small-size and Vertically positioned, in the following figures); the grid is plotted at eight gridlines in the circumferential direction and four gridlines in the radial direction for clarity.

2.2. Numerical Methods

The thermal and flow patterns are governed by the two-dimensional equations of mass, momentum, and energy:

$$\nabla \cdot \mathbf{u} = 0, \tag{1}$$

$$\frac{\partial \mathbf{u}}{\partial t} + (\mathbf{u} \cdot \nabla)\mathbf{u} = -\nabla p + \sqrt{\frac{Pr}{Ra}}\nabla^2 \mathbf{u} + (0, T)^T, \tag{2}$$

$$\frac{\partial T}{\partial t} + (\mathbf{u} \cdot \nabla)T = \sqrt{\frac{1}{PrRa}}\nabla^2 T. \tag{3}$$

The variables were scaled by the reference length, D_o; velocity, $u_{ref} = (a/D_o)(PrRa)^{1/2}$; pressure, $p_{ref} = pu_{ref}^2$; and time, D_o/u_{ref}. The temperature was scaled as $T = (T^* - T_o)/(T_i - T_o)$, where T^* is the dimensional temperature. A no-slip and no-penetrating condition was applied for the velocity components on all solid walls, and the temperature was $T = 1$ for the plate and $T = 0$ for the enclosure. Although the geometry is left-right symmetric about the vertical centerline ($x/D = 0.0$) for all simulations in this work, we chose to discretize the whole computational domain, instead of half of the domain with the symmetric condition at the vertical centerline, to avoid failure in capturing any possible oscillatory flow behaviors.

The above governing equations were solved by our in-house finite-difference code, which has been employed and well validated in our earlier works for steady-state natural convection in an enclosure [9,18], transient or unsteady mixed convection in an enclosure [19,20], and forced convection across cylinders [21–26]. The numerical details are omitted here for simplicity. In this work, we validated the code through the physical problem of natural convection in an annulus consisting of two concentric circular cylinders at $Ra = 1.71 \times 10^6$, which was experimentally and numerically studied by Kuehn and Goldstein [27] and detailed quantitative benchmark results were provided. This configuration had the same geometric topology as the one in our simulation. The mean equivalent conductivity coefficient was defined as the ratio between the heat transfer rate of the convection case and pure conduction case:

$$k_{eq} = \frac{Nu_{avg,conv}}{Nu_{avg,cond}}, \tag{4}$$

in which the mean Nusselt number was computed as:

$$Nu_{avg} = \frac{1}{\partial\Omega} \int_{\partial\Omega} Nu \, d\partial\Omega,$$ (5)

where $\partial\Omega$ is the surface area of the enclosure or plate. The thermal conductivity coefficient reflects the additional heat transfer provided by fluid circulation in addition to conduction and is an indicator of the convection intensity. The value of k_{eq} obtained under various resolutions is given in Table 2. Our results are in good agreement with the benchmark experimental results. The coefficient obtained under various resolutions does not show much difference, i.e., a relative difference of less than 0.2% between the results obtained at the 256 × 128 and 512 × 256 grid, thus the 512 × 256 grid was deemed sufficient for this simulation.

Table 2. Mean equivalent conductivity coefficient obtained under various resolutions at $Ra = 1.71 \times 10^6$ against the numerical results by Kuehn and Goldstein.

Source	Mesh	$k_{eq,i}$	$k_{eq,o}$
Kuehn and Goldstein	16 × 19	3.024	2.973
Present	128 × 64	2.972	2.981
	256 × 128	2.961	2.967
	512 × 256	2.958	2.962

In this work, we performed a grid sensitivity study for the $H{\cdot}W/D^2 = 0.04$ cases with a square cylinder ($H/D = W/D = 0.2$), a vertically placed plate with H/D = 0.8, and a horizontally placed plate with $W/D = 0.8$ using the 256 × 256, 512 × 256, and 512 × 512 grids following the manner described in [28,29]. The computed mean Nusselt numbers on the enclosure surface are given in Table 3. It is seen that the maximum relative difference of the Nusselt number computed under the 256 × 256 and 512 × 256 is relatively large, while the maximum difference between the results of the 512 × 256 and 512 × 512 grid is only about 0.6%. The 512 × 256 grid was found to fine enough and was used in all simulations. The size of the first-layer grid in the wall-normal direction on the plate surface was around 0.0005D with clustering at the sharp corners, and was around 0.001D on the enclosure surface.

Table 3. Mean Nusselt number $Nu_{avg,o}$ for the H·$W/D^2 = 0.04$ case under different resolutions.

Resolution	H/D = W/D = 0.2	H/D = 0.8	W/D = 0.8
256 × 256	3.965	6.574	5.134
512 × 256	4.102	6.699	5.367
512 × 512	4.125	6.705	5.379

3. Results and Discussion

3.1. Mean Heat Transfer

The heat transfer performance of the plate-enclosure system was first assessed by the mean heat transfer rate. In Figure 2a, the mean Nusselt number is presented for the enclosure. In general, Nu_{avg} monotonically increases with the cross-section area of the plate, and the value for the vertical plate cases is larger than that of the horizontal plate cases. A further inspection on the variations shows that for the vertical plate, Nu_{avg} increases rapidly with H, while the increase with W for the horizontal plate is notably minor, especially for plates with a large cross-section area, e.g., almost constant Nu_{avg} for the $H{\cdot}W/D^2 = 0.09$ plate, which is nearly the same as the square plate. This mild variation demonstrates that for a horizontal plate with a large cross-section area, the aspect ratio has tiny effects on Nu_{avg}. However, the mean heat transfer rate is still larger for plates with a large W considering that the surface area changes with the aspect ratio. The variation of the mean Nusselt number for the plate is shown in Figure 2b, which was computed using the same approach as in Equation (5). This subfigure

demonstrates the efficiency of the heat transfer in terms of the unit surface area of the plate. It is easily demonstrated that with the increases of *H* or *W*, both the mean heat transfer rate and surface area increase, while the heat transfer rate per area, i.e., Nu_{avg}, decreases as the increase of the surface area is not so efficient in enhancing heat transfer. It is seen in the subfigure that for a vertical plate, the plate with a smaller cross-section area has a higher Nu_{avg} because of the reduced surface area at the top and bottom where heat transfer is not efficient; however, for a horizontal plate, the increase of *W* has a negligible effect, which indicates that we can simply enhance heat transfer by employing a thick plate.
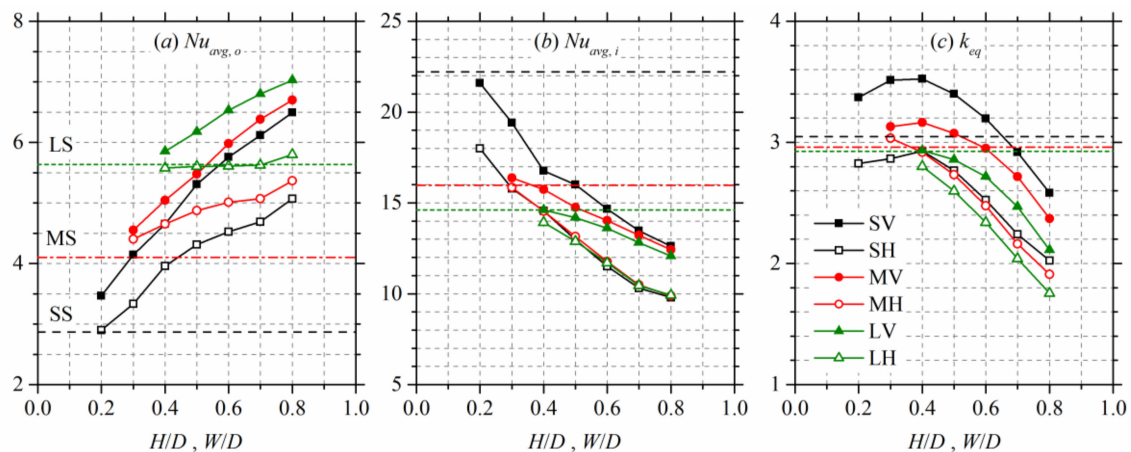

Figure 2. Variations of characteristic quantities: (**a**) mean Nusselt number on the enclosure surface; (**b**) mean Nusselt number on the plate surface; (**c**) mean equivalent conductivity coefficient.

Figure 2c gives the variation of the equivalent thermal conductivity coefficient. Since the fluid is driven by the temperature difference, the convection heat transfer is mainly affected by two factors: The surface area of the plate that heats the adjacent fluid, and the confinement of the plate on the circulation of fluid, which weakens the heat transfer. The combined effect of the two factors determines the convection intensity. For the square geometry (*H* = *W*), the value of k_{eq} slightly decreases with the cross-section area, which indicates that the large surface area for heating cannot compensate the weakening of the fluid circulation due to the confinement from the plate. It is noticed that the curves in the subfigure exhibit non-monotonic variation with *H* or *W*. For the vertical plate, the value of k_{eq} presents an increasing-decreasing pattern with increasing H for plates with $H \cdot W/D^2 = 0.01$ and 0.04, while it monotonically decreases with H for the $H \cdot W/D^2 = 0.09$ geometry. In conclusion, the increase of *H* or *W* generally provides less contribution to the convection heat transfer.

3.2. Thermal and Flow Patterns

To further exhibit the effects of the orientation and aspect ratio of the flat plate on the heat transfer mechanism, Figures 3–5 present the distributions of the stream function and temperature in the fluid domain for plates of various cross-section areas. Both distributions are left-right symmetric about the vertical centerline due to the symmetric configuration, thus we gave the isolines of the stream function in the left half of the figure, which coincide with the streamlines, and isotherms in the right half of the enclosure. For the smallest cross-section area, $H \cdot W/D^2 = 0.01$, the plate with a large *H* has two long surfaces, which could intensely heat the adjacent fluid, thus a primary vortex forms besides the plate, which recirculates within almost the whole enclosure; moreover, the fluid at the center of the vortex is only weakly driven by the temperature difference and the shear stress breaks the vortex into two smaller ones. It is noticed that for a plate with *H/D* = 0.8, the intensity of fluid recirculation to both sides of the plate is strong, and a small and weak vortex that rotates in the clockwise (CW) direction appears at the top of the enclosure. As *H* decreases, the primary vortex shrinks in size roughly along the vertical direction and the fluid close to the bottom of the enclosure is less affected; the shrinking vortex does not break into multiple ones at its center. The isotherms mainly present a stratification structure. For the

horizontal plate, the circulation of fluid within the enclosure is confined by the plate and exhibits complex structures. There is only one primary vortex to the bottom of the plate at $W/D = 0.2$–0.3; as W increases, the end of the plate separates the primary vortex into two at $W/D = 0.4$–0.7, with one CW rotating vortex entirely above the plate and one counterclockwise (CCW) rotating vortex beside and below it. For the longest plate at $W/D = 0.8$, the CCW vortex is separated into two smaller individual ones. Since the fluid below the plate is less driven by the buoyancy, the fluid circulation is strong above the plate and is dominated by the CW vortex. It is seen from the isotherms that for the long horizontal plate ($W/D = 0.4$–0.8), the thermal plume structure forms at the end whose direction is approximately along the boundary between the CW and CCW vortices.
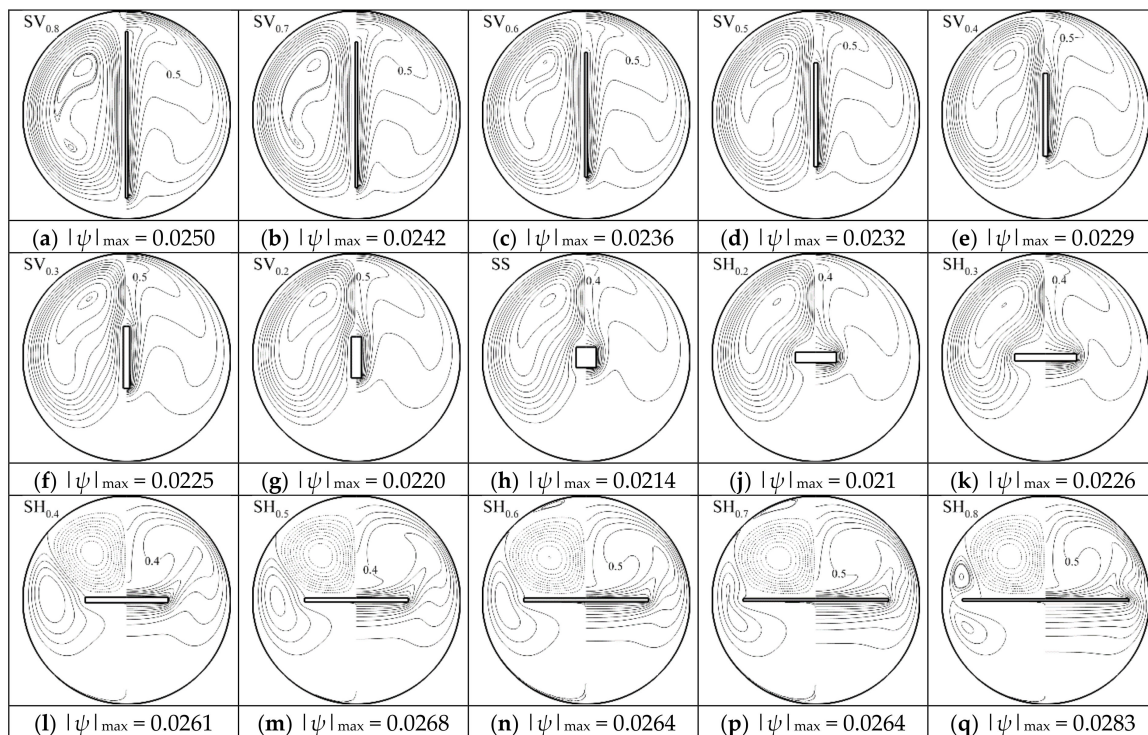

Figure 3. Fields of streamlines (left semicircle) and isotherms (right semicircle) for the small-sized plate ($H \cdot W/D^2 = 0.01$). The isolines of the stream function are plotted approximately at $\Delta\psi = 0.1|\psi_{max} - \psi_{min}|$; the solid lines are for the counterclockwise rotating vortex and the dashed lines are for clockwise rotating vortex. The isotherms are plotted at $\Delta T = 0.1$.

As the cross-section area increases, the thickness of the plate will also increase for all lengths. The increased thickness has two significant effects on the thermal and flow patterns. The first effect is that the fluid adjacent to the short surface of the plate is more notably heated. It is seen in Figure 4 that the enhanced heating on the fluid generates the CW vortex at the top of the plate at $H/D = 0.6$–0.8, whose size is larger than that of the $H \cdot W/D^2 = 0.01$ cases; as H decreases, the upward circulating flow above the plate is relatively weaker since the plate is far from the top of the enclosure, thus the CW vortex diminishes. Moreover, there is one small CW vortex just above the plate at $H/D = 0.3$–0.5 because of the separation of upward flow at the sharp corners of the plate. The second effect resulting from the increased thickness is the separation of the primary vortex by the end of the horizontal plate. There is always one CW vortex above the plate, and two CCW vortices in the gap region between the end of the plate and the enclosure, or even three CCW vortices at $W/D = 0.8$–0.9. The effect of the thick plate on the isotherms is the thermal plume structures at the top sharp corners, which is observable for all horizontal plate cases. The above two effects are more remarkable for the $H \cdot W/D^2 = 0.09$ case as shown in Figure 5; the CW vortex above the plate always exists and dominates the circulating flow for the horizontal plate cases, and the thermal plume structure at the sharp corners persists.
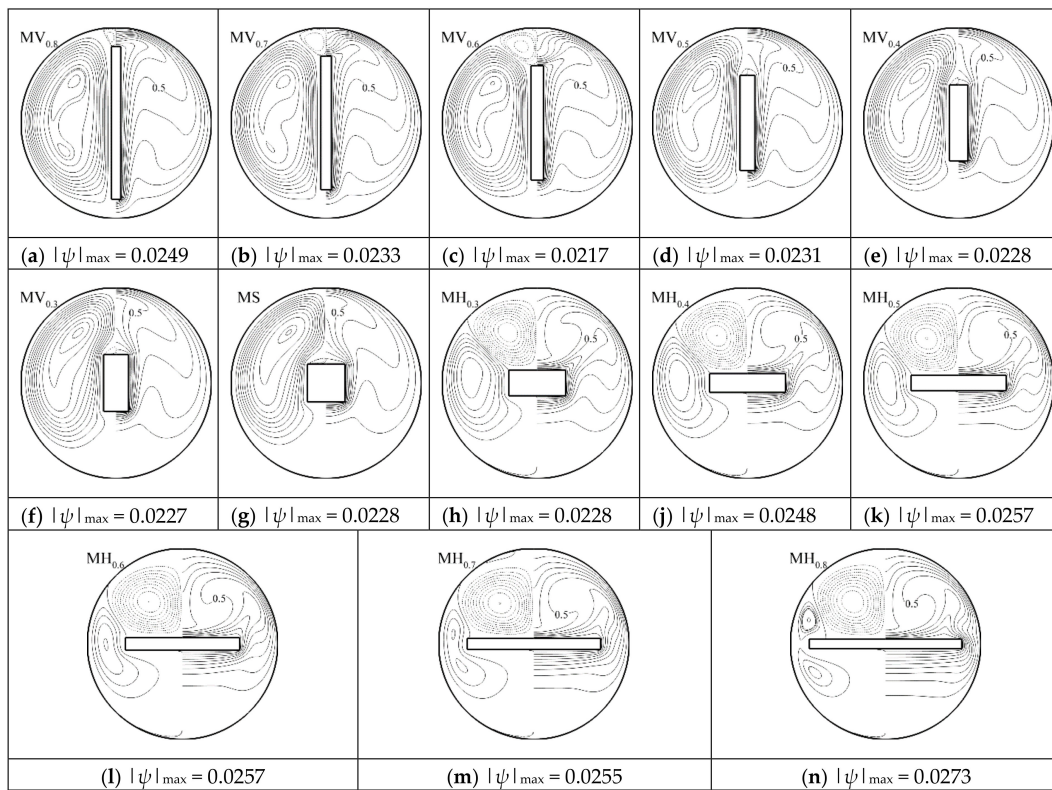
Figure 4. Fields of streamlines (left semicircle) and isotherms (right semicircle) for the middle-sized plate ($H \cdot W/D^2 = 0.04$). The isolines are plotted the same as in Figure 3.
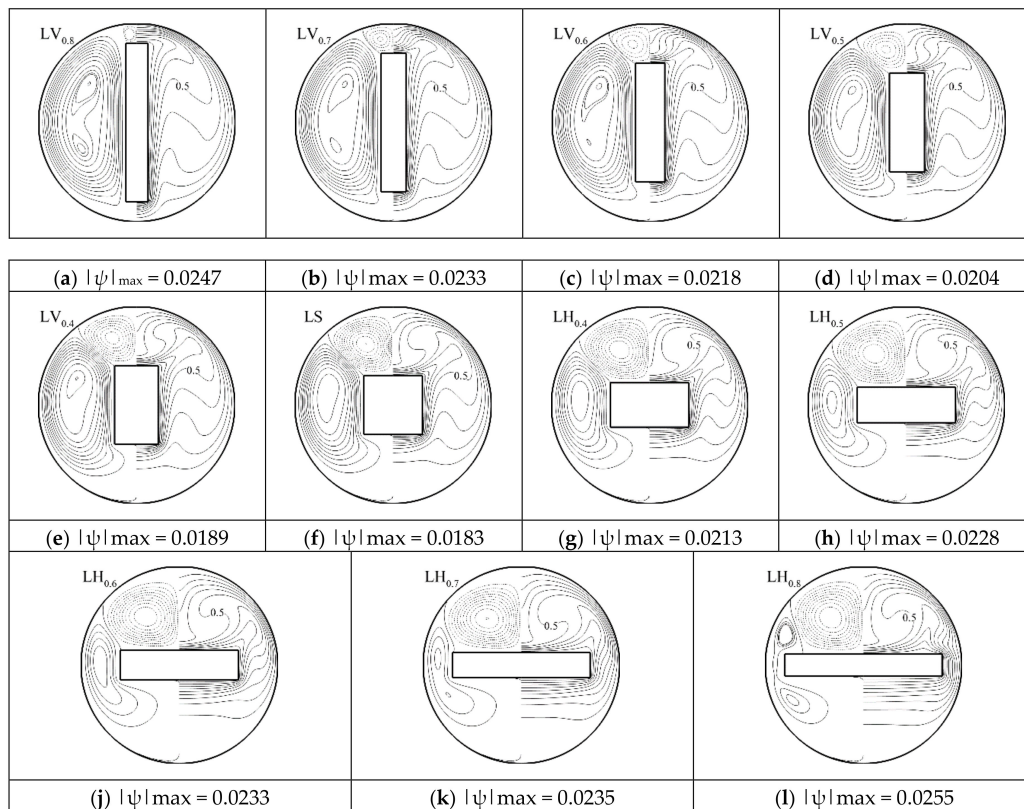

Figure 5. Fields of streamlines (left semicircle) and isotherms (right semicircle) for the middle-sized plate ($H \cdot W/D^2 = 0.04$). The isolines are plotted the same as in Figure 3.

3.3. Local Heat Transfer

The temperature distribution affected by the formation of various vortices would influence the heat transfer on the solid walls and may determine the performance of the plate-enclosure system in certain engineering applications. Figure 6 presents the distribution of the local Nusselt number in the circumferential direction on the wall of the enclosure. Considering the symmetric configuration and temperature field, only the curves for the right half of the enclosure were plotted with the circumferential angle, as given in Figure 1, and the left and right columns of the subfigures denote the vertical and horizontal plate cases, respectively. For the vertical plate, it is obviously seen that the magnitude of the local Nusselt number gradually decreases with the decreasing H for the majority of the enclosure. For the $H \cdot W/D^2 = 0.01$ plate, there is a bump at $\theta = 10°–20°$ for the $H/D = 0.6–0.8$ configurations because of the small gap between the sharp corners of the plate and the enclosure, and it vanishes for $H/D \leq 0.5$ because the end of the plate is relatively far away from the enclosure. It is also noticed that the magnitude of the local Nusselt number at the top of the enclosure does not occur for the longest plate at $H/D = 0.8$ because the fluid above the plate is confined and local heat transfer is conduction dominant, while the circulating flow enhances the heat transfer for plates with a reduced length. The small gap for the longest plate also results in the bump at the bottom of the enclosure. For the plate with a cross-section area of $H \cdot W/D^2 = 0.04$, three differences are observed compared with the results of the $H \cdot W/D^2 = 0.01$ cases. The first is the larger amplitude of the local Nusselt number variation, with H at the top of the enclosure; the second is the bump observed for the $H/D = 0.5$ plate; and the third is the non-monotonic variation of the local Nusselt number, especially in the region of $\theta < 80°$, which is mainly attributed to the clustered isotherms because of the thicker plate. For the plate of $H \cdot W/D^2 = 0.09$, the fluid in the gap to the top of the plate is always dominated by the weak secondary vortex, thus the magnitude of the local Nusselt number is reduced. The thick plate also reduces the gap size and induces the bump on all curves because of the thermal plume structure, and a higher local Nusselt number at the bottom of the enclosure.

For the horizontal plate, the variation of the local Nusselt number with W is more complex because it is dependent on the various vortices. For the $H \cdot W/D^2 = 0.01$ plate at $W/D = 0.2–0.3$, the Nusselt number at the top of the enclosure is large because of the strongly circulating primary vortex. However, as W increases, the magnitude of the Nusselt number abruptly reduces since the secondary vortex is relatively weak and the heat transfer at the enclosure top is not so intense, and a bump is observed on the curve because of the thermal plume; a second bump at $\theta = 95°$ occurs due to the conduction in the small gap. For the $H \cdot W/D^2 = 0.04$ and 0.09 plates, since the secondary vortex and thermal plume exist for all lengths, a local maximum around $\theta = 60°$ is always observed on the curves, which corresponds to the thermal plume. In general, for the horizontal plate, the plate length, *W*, has a minor effect on the local Nusselt number roughly in the region $\theta < 60°$, while the interaction of CW and CCW vortices and the separation of the primary vortex by the end of the plate in the region $\theta > 60°$ complicate the local flow pattern, thus the effect of W on the local Nusselt number is also more pronounced.

The orientation and aspect ratio of the plate also affect the heat transfer characteristics on the surface of the plate. Figure 7 gives the distribution of the local Nusselt number on the plate, in which the local coordinate, s, is depicted in Figure 1. It is summarized that there is always a peak at the sharp corners of the plate, which can be one order of magnitude higher than that of the flat surface, and the magnitude of the Nusselt number is relatively higher at the bottom of the plate due to the fluid circulation. For the vertical plate, the Nusselt number generally increases with decreasing H, and the differences between the several curves get smaller as the cross-section area increases. For the horizontal plate, the secondary vortex possibly forming above the plate reduces the local Nusselt number in the region, $s < 0.2$, which corresponds to the sharp top corner. As W increases, the magnitude of the Nusselt number for the top and bottom surfaces nearly monotonically decreases because of the confinement of the plate on the fluid circulation.
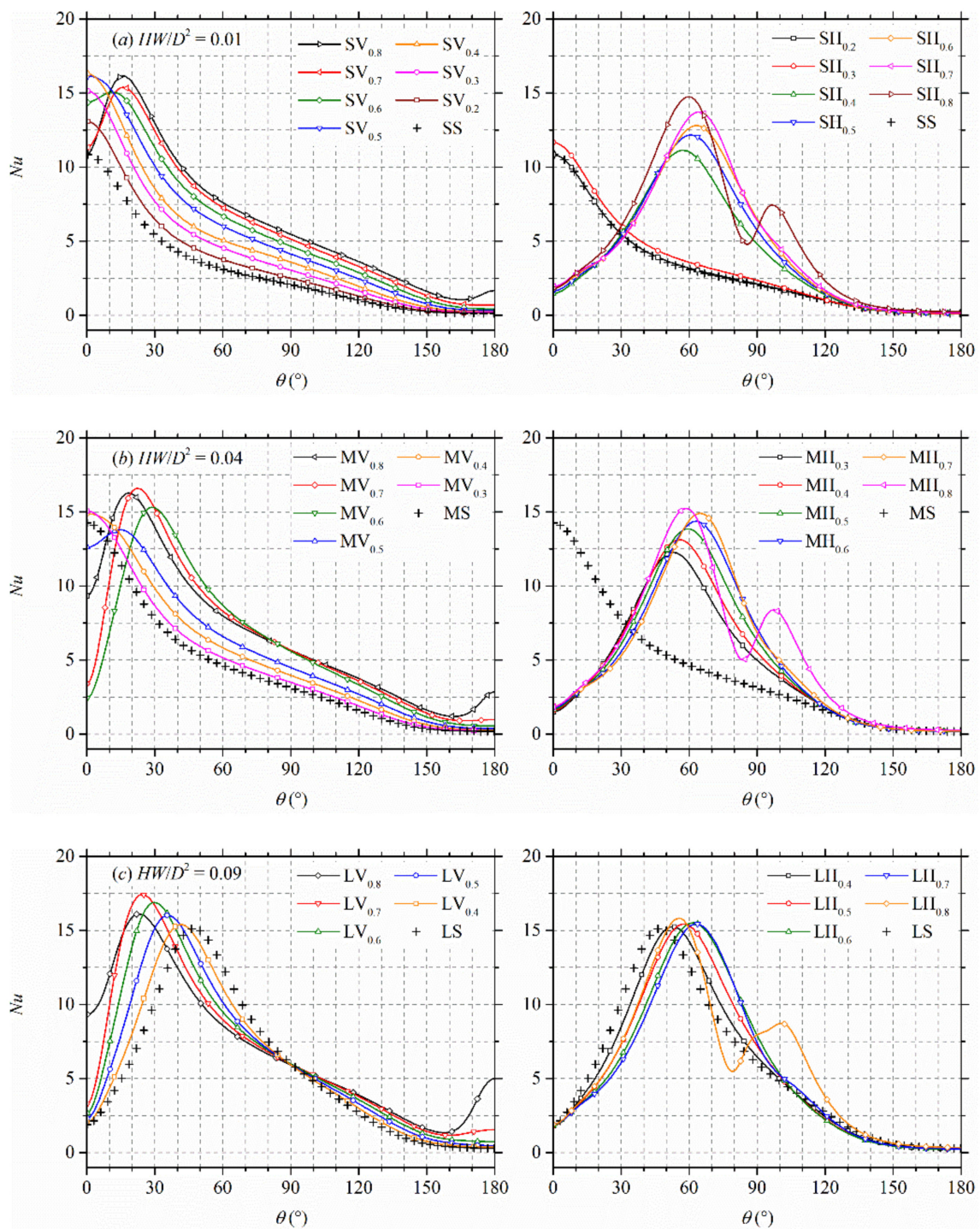
Figure 6. Circumferential distribution of the local Nusselt number on the enclosure surface.
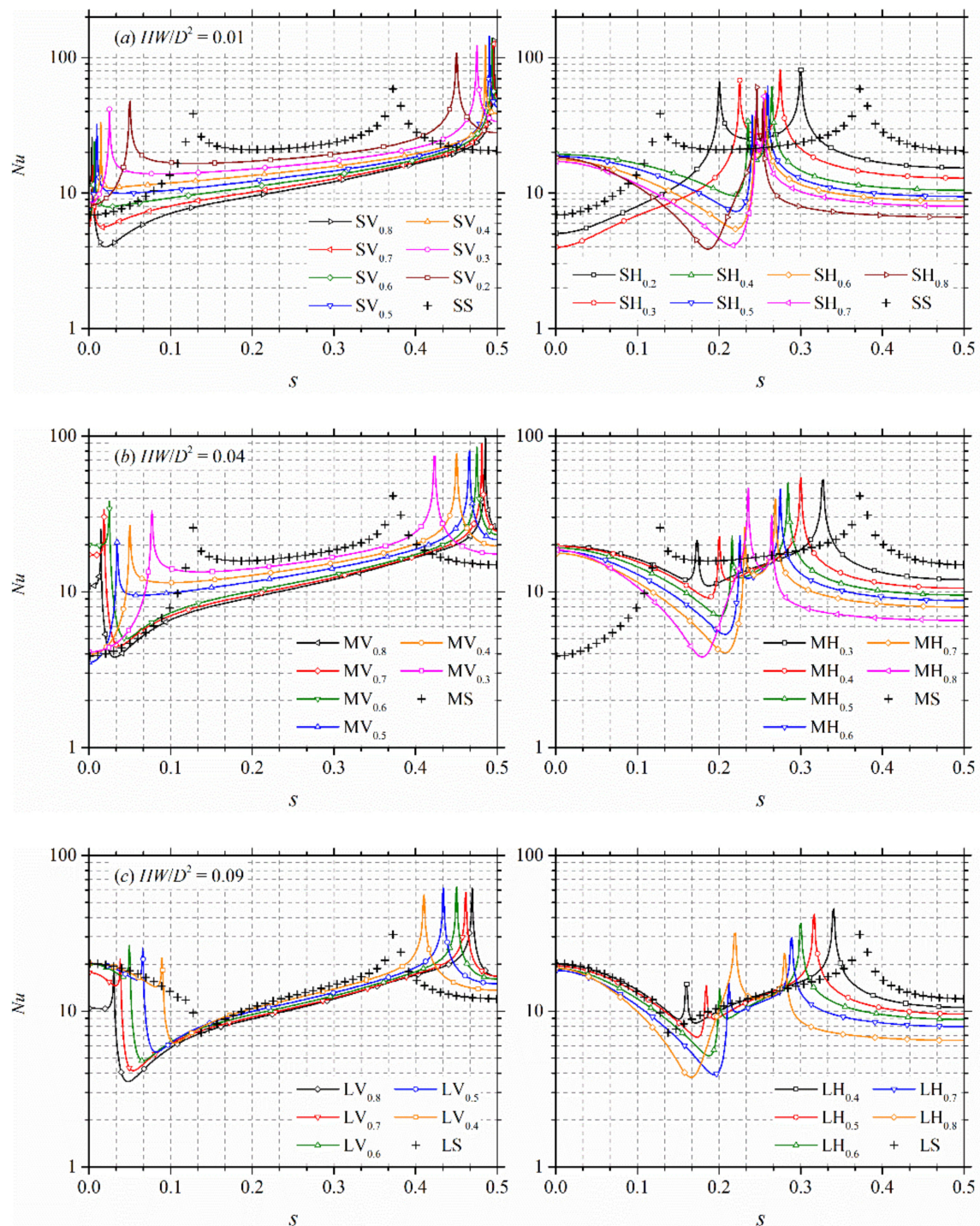
Figure 7. Circumferential distribution of the local Nusselt number on the plate surface.

3.4. Synergy Principle Analysis

The enhancement of heat transfer contributed by convection with respect to pure conduction is a result of the circulation of fluid within the enclosure. Quantitative analysis of the enhancement is significant in understanding the related physics. Since the fluid moves in parallel with the solid wall in the boundary layer region, the fluid-solid heat transfer is realized almost by pure conduction. However, in the fluid domain outside of the boundary region, the intensity of heat transfer is dependent on the direction of flow considering the non-uniform temperature distribution, i.e., the alignment of the vectors of the velocity and temperature gradient. The heat transfer is enhanced if the velocity vector is

aligned in the direction with the temperature gradient in which the fluid circulation could effectively mix the hot and cold fluid and increase the local heat transfer rate. Guo et al. [30] proposed the field synergy principle:

$$\mathbf{U} \cdot \nabla T = |\mathbf{U}||\nabla T| \cos \beta, \tag{6}$$

in which β represents the synergy angle between the two vectors. The local heat transfer can be enhanced if the two vectors are synergized.

We computed the synergy coefficient, $\cos\beta$, for this problem and present its distribution in Figure 8. In general, for the vertically placed plate, the value of $\cos\beta$ is almost zero at the solid walls, which indicates that the local heat transfer is conduction dominant. The enhancement of heat transfer from convection mainly occurs in the central region of the fluid domain and exhibits a zigzag structure with a relatively large magnitude, thus the local heat transfer from the mixing of cold and hot fluid is intense. The magnitude of the synergy coefficient to the top of the plate is also large, especially for plates with a larger cross-section area, which is attributed to the formation of the CW vortex and thermal plume structure. It is also noticed that due to the existence of the CW vortex, the direction of the fluid motion is reversed from upward for the $H \cdot W/D^2 = 0.01$ case to downward for the $H \cdot W/D^2 = 0.04$ and 0.09 cases, thus the magnitude for the local synergy coefficient is also changed. A similar distribution pattern is also observed for the horizontally placed plate. However, due to the formation of multiple CW and CCW vortices in the gap region between the end of the plate and the enclosure, the distribution of $\cos\beta$ is even more complex. Since the CW vortex dominates the flow above the plate, the magnitude of $\cos\beta$ is large at the vortex center and its boundary where the thermal plume appears. The effect of the plate length is noticeable mainly in the gap region, where the CCW vortex is separated by the plate; it has only one local maximum at the center of the vortex for the relatively short plate where there is one CCW vortex, while two local maxima are observed as the CCW vortex is separated by the long plate into two.
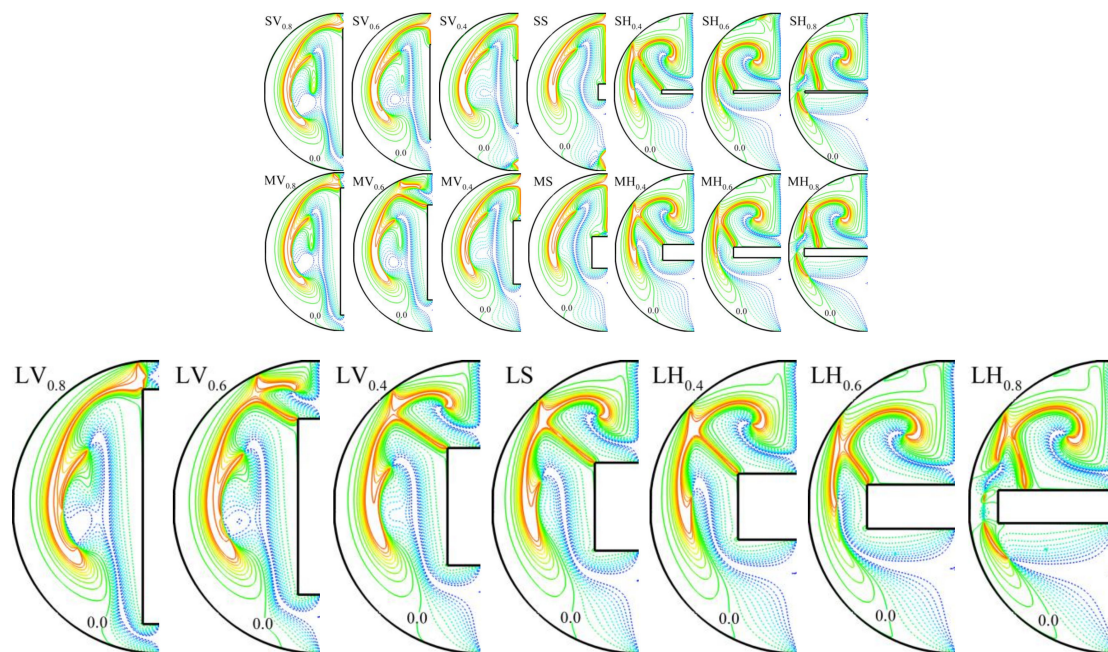

Figure 8. Field of synergy coefficient plotted at $\cos\beta = [-1.0, 1.0]$ with $\Delta\cos\beta = 0.1$. The solid and dashed lines respectively denote the positive and negative values.

4. Conclusions

This work performed a numerical investigation on the natural convection in a circular enclosure with an internal flat plate of a constant cross-section area but different orientation and aspect ratio.

For this physical problem, we first explored the trade-off between the height and width of the plate under the constraint of a fixed cross-section area by considering the effects of the heating surface area and fluid circulating confinement, since the heat transfer effectiveness is greatly dependent on these two factors. The numerical results led to the following conclusions:

(1) The vertically placed plate produces significant convection heat transfer with a higher mean Nusselt number than the horizontal plate. However, the overall heat transfer rate does not vary much with the width of the plate for the horizontally placed plate cases.

(2) For the vertically placed plate, there is always one primary vortex to each side of the plate, and one secondary vortex may form above the plate as the width increases, especially for plates with larger cross-section areas. For the horizontally placed plate with a large width, the primary vortex can be separated by the end of the plate into two, and a secondary vortex forms above the plate.

(3) The magnitude of the local heat transfer rate on the enclosure surface is higher as the circulating flow impinges on the surface, and it is normally maximum at the circumferential position of the thermal plume. The secondary vortex above the plate actually reduces the local heat transfer rate at the top of the enclosure.

(4) A field synergy analysis revealed that the contribution of fluid circulation to the convection heat transfer mainly appears at the center of the vortices, at the boundary of neighboring vortices where the thermal plume forms, and above the plate.

The present work performed more of a theoretical study on the natural convection in an enclosure with a specific geometric configuration. However, considering that the flat plate geometry is widely used in engineering applications, the findings and conclusions could provide a useful guidance or reference for other applications in choosing the proper geometry and orientation to maximize heat transfer effectiveness.

Author Contributions: Conceptualization, A.W. and W.Z.; Data curation, A.W.; Formal analysis, A.W.; Funding acquisition, L.Z. and W.Z.; Investigation, A.W., C.Y., Y.W., L.Y. and Y.Y.; Methodology, W.Z.; Project administration, L.Z. and W.Z.; Resources, L.Z. and W.Z.; Software, W.Z.; Supervision, L.Z. and W.Z.; Validation, A.W.; Visualization, A.W.; Writing—Original draft, A.W.; Writing—Review and editing, W.Z.

References

1. Alteç, Z.; Kurtul, Ö. Natural convection in tilted rectangular enclosures with a vertically situated hot plate inside. *Appl. Therm. Eng.* **2007**, *27*, 1832–1840. [CrossRef]

2. Wang, X.; Shi, D.; Li, D. Natural convective flow in an inclined lid-driven enclosure with a heated thin plate in the middle. *Int. J. Heat Mass Trans.* **2012**, *55*, 8073–8087. [CrossRef]

3. Öztop, H.F.; Dagtekin, I.; Bahloul, A. Comparison of position of a heated thin plate located in a cavity for natural convection. *Int. Commun. Heat Mass Trans.* **2004**, *31*, 121–132. [CrossRef]

4. Tasnim, S.H.; Collins, M.R. Suppressing natural convection in a differentially heated square cavity with an arc shaped baffle. *Int. Commun. Heat Mass Trans.* **2005**, *32*, 94–106. [CrossRef]

5. Wang, Q.W.; Yang, M.; Tao, W.Q. Natural convection in a square enclosure with an internal isolated vertical plate. *Warme Stoffubertrag* **1994**, *29*, 161–169. [CrossRef]

6. Abdul Hakeem, A.K.; Saravanan, S.; Kandaswamy, P. Buoyancy convection in a square cavity with mutually orthogonal heat generating baffles. *Int. J. Heat Fluid Flow* **2008**, *29*, 1164–1173. [CrossRef]

7. Kandaswamy, P.; Abdul Hakeem, A.K.; Saravanan, S. Internal natural convection driven by an orthogonal pair of differentially heated plates. *Comput. Fluids* **2015**, *111*, 179–186. [CrossRef]

8. Singh, P.; Liburdy, J.A. Effect of plate inclination on natural convection from a plate to its cylindrical enclosure. *ASME J. Heat Transf.* **1986**, *108*, 770–775. [CrossRef]

9. Zhang, W.; Wei, Y.; Chen, X.; Dou, H.-S.; Zhu, Z. Partitioning effect on natural convection in a circular enclosure with an asymmetrically placed inclined plate. *Int. Commun. Heat Mass Trans.* **2018**, *90*, 11–22. [CrossRef]

10. Dagtekin, I.; Öztop, H.F. Natural convection heat transfer by heated partitions within enclosure. *Int. Commun. Heat Mass Trans.* **2001**, *28*, 823–834. [CrossRef]

11. Nag, A.; Sarkar, A.; Sastri, V.M.K. Natural convection in a differentially heated square cavity with a horizontal partition plate on the hot wall. *Comput. Method Appl. Mech. Eng.* **1993**, *110*, 143–156. [CrossRef]

12. Tasnim, S.H.; Collins, M.R. Numerical analysis of heat transfer in a square cavity with a baffle on the hot wall. *Int. Commun. Heat Mass Trans.* **2004**, *31*, 639–650. [CrossRef]

13. Sun, C.; Yu, B.; Öztop, H.F.; Wang, Y.; Wei, J. Control of mixed convection in lid-driven enclosures using conductive triangular fins. *Int. J. Heat Mass Trans.* **2011**, *54*, 894–909. [CrossRef]

14. Wei, Y.; Yang, H.; Dou, H.-S.; Lin, Z.; Wang, Z.; Qian, Y. A novel two-dimensional coupled lattice Boltzmann model for thermal incompressible flows. *Appl. Math. Comput.* **2018**, *339*, 556–567. [CrossRef]

15. Lun, Y.X.; Lin, L.M.; Zhu, Z.C.; Wei, Y.K. Effects of vortex structure on performance characteristics of a multiblade fan with inclined tongue, P.I. *Mech. Eng. Part A* **2019**, *233*, 1007–1021. [CrossRef]

16. Yang, H.; Yu, P.; Xu, J.; Ying, C.; Cao, W.; Wang, Y.; Zhu, Z.; Wei, Y. Experimental investigations on the performance and noise characteristics of a forward-curved fan with the stepped tongue. *Meas. Control* **2019**, in press. [CrossRef]

17. Tao, J.; Lin, Z.; Ma, C.; Ye, J.; Zhu, Z.; Li, Y.; Mao, W. An experimental and numerical study of regulating performance and flow loss in a V-port ball valve. *J. Fluids Eng.* **2020**, *142*, 021207. [CrossRef]

18. Wang, Y.; Chen, J.; Zhang, W. Natural convection in a circular enclosure with an internal cylinder of regular polygon geometry. *AIP Adv.* **2019**, *9*, 065023. [CrossRef]

19. Zhang, W.; Wei, Y.; Dou, H.-S.; Zhu, Z. Transient behaviors of mixed convection in a square enclosure with an inner impulsively rotating circular cylinder. *Int. Commun. Heat Mass Trans.* **2018**, *98*, 143–154. [CrossRef]

20. Yang, H.; Zhang, W.; Zhu, Z. Unsteady mixed convection in a square enclosure with an inner cylinder rotating in a bi-directional and time-periodic mode. *Int. J. Heat Mass Trans.* **2019**, *136*, 563–580. [CrossRef]

21. Zhang, W.; Chen, X.; Yang, H.; Liang, H.; Wei, Y. Forced convection for flow across two tandem cylinders with rounded corners in a channel. *Int. J. Heat Mass Trans.* **2019**, *130*, 1053–1069. [CrossRef]

22. Zhang, W.; Yang, H.; Dou, H.-S.; Zhu, Z. Forced convection of flow past two tandem rectangular cylinders in a channel. *Numer. Heat Tr. Part A* **2017**, *72*, 89–106. [CrossRef]

23. Zhang, W.; Li, X.; Zhu, Z. Quantification of wake unsteadiness for low-Re flow across two staggered cylinders, P.I. *Mech. Eng. Part C* **2019**, *233*, 6892–6909. [CrossRef]

24. Zhang, W.; Dou, H.-S.; Zhu, Z.; Li, Y. Unsteady characteristics of low-Re flow past two tandem cylinders. *Theor. Comput. Fluid Dyn.* **2018**, *32*, 475–493. [CrossRef]

25. Zhang, W.; Samtaney, R. Effect of corner radius in stabilizing the low-Re flow past a cylinder. *J. Fluids Eng.* **2017**, *139*, 121202. [CrossRef]

26. Zhang, W.; Yang, H.; Dou, H.-S.; Zhu, Z. Flow unsteadiness and stability characteristics of low-Re flow past an inclined triangular cylinder. *J. Fluids Eng.* **2017**, *139*, 121203. [CrossRef]

27. Kuehn, T.H.; Goldstein, R.J. An experimental and theoretical study of natural convection in the annulus between horizontal concentric cylinders. *J. Fluid Mech.* **1976**, *74*, 695–719. [CrossRef]

28. Siddique, W.; El-Gabry, L.; Shevchuk, I.V.; Hushmandi, N.B.; Fransson, T.H. Flow structure, heat transfer and pressure drop in varying aspect ratio two-pass rectangular smooth channels. *Heat Mass Transf.* **2012**, *48*, 735–748. [CrossRef]

29. Siddique, W.; Shevchuk, I.V.; El-Gabry, L.; Hushmandi, N.B.; Fransson, T.H. On flow structure, heat transfer and pressure drop in varying aspect ratio two-pass rectangular channel with ribs at 45°. *Heat Mass Transf.* **2013**, *49*, 679–694. [CrossRef]

30. Guo, Z.Y.; Tao, W.Q.; Shah, R.K. The field synergy (coordination) principle and its applications in enhancing single phase convective heat transfer. *Int. J. Heat Mass Transf.* **2005**, *48*, 1797–1807. [CrossRef]